Impact of propagation effects on intersubband Rabi flopping in semiconductor quantum wells

Xusheng Zhou (周旭升), Ni Cui (崔 妮), Jifeng Zu (祖继锋), and Shangqing Gong (龚尚庆)

Shanghai Institute of Optics and Fine Mechanics, Chinese Academy of Sciences, Shanghai 201800

Received March 28, 2008

We investigate intersubband Rabi flopping in modulation-doped semiconductor quantum wells with and without the propagation effects, respectively. It is shown that propagation effects have a larger impact on Rabi flopping than the nonlinearities rooted from electron-electron interactions in multiple quantum wells. By using ultrashort π pulses, an almost complete population inversion exists if the propagation effects are not considered; while no complete population inversion occurs in the presence of propagation effects. Furthermore, the magnitude of the impact of propagation effects may be controlled by varying the carrier density.

OCIS codes: 040.4200, 140.0140, 190.0190, 320.0320.
doi: *10.3788/COL20080609.0689.*

Nowadays, the phenomena closely allied with two-level atomic Rabi flopping[1−4] have been observed in semiconductors, which provide an approximate realization of two-level systems[5−8]. Furthermore, there are already considerable interests in Rabi flopping involving interband dynamics of low-dimensional semiconductor, such as quantum wells(QWs)[3,9] and quantum dots[10,11]. Recently, the interest in Rabi flopping extends to intersubband (IS) systems of semiconductor QWs[12−16]. In most of these studies, the optical response and the electron dynamics of IS transitions in QWs can be significantly effected by many-body effects due to the macroscopic carrier density. However, for a multiple QW system, the propagation effects should be considered in the study of the coherent dynamics of radiatively coupled QW excitons[17] and electrons[18]. Waldmueller *et al.*[19] have shown the radiative coupling which has a large impact on Rabi oscillations of subband populations by using a many-partical theory including light propagation effects with Green function.

In a particular study on a modulation-doped symmetric double semiconductor QWs, Olaya-Castro *et al.*[20] have derived the effective Bloch equations describing the effects of electron-electron interactions on IS transitions. Considering the strong nonlinearities rooted from macroscopic electron density, Paspalakis *et al.*[21] have presented conditions that could lead to complete inversion in the system for a wide range of parameters. In this paper, we investigate the IS Rabi flopping in multiple symmetric double QWs with and without the propagation effects, respectively by solving the effective nonlinear Bloch equations of Olaya-Castro *et al.*[20] and the full Maxwell's wave equations. From our numerical results with π pulses in the absence of propagation effects, an almost complete population inversion exists. While in the present of propagation effects, the Rabi flopping is suppressed due to propagation effects and electron-electron interaction, and the complete population inversion is impossible.

We consider a n-type modulation-doped multiple QWs sample consisting of N equally spaced electronically uncoupled symmetric double semiconductor GaAs/AlGaAs QWs with separation d, which was shown in Ref. [20]. There are only two lower energy subbands contribute to the system dynamics, $n = 0$ for the lowest subband with even parity and $n = 1$ for the excited subband with odd parity. The Fermi level is below the $n = 1$ subband minimum, so the excited subband is initially empty. This is succeeded by a proper choice of the electron sheet density. The two subbands are coupled by a time-dependent laser pulse along the z axis, which is described by $E_x(z = 0, t) = \varepsilon_0 \mathrm{sech}[1.76(t - t_0)/\tau_\mathrm{p}] \cos[\omega(t - t_0)]$, where ε_0 is the electric field amplitude, ω is the central carrier frequency, τ_p is the full-width at half-maximum of the pulse intensity envelope of the laser pulse, and t_0 is the delay.

We consider the propagation property of an ultrashort laser pulse $E_x(z, t)$ along the z axis in the multiple double symmetric QWs. With the constitute relation for the electric displacement for the polarization along the x axis, the Maxwell's wave equations for the medium take the form:

$$\partial_t H_y = -\frac{1}{\mu}\partial_z E_x, \tag{1}$$

$$\partial_t E_x = -\frac{1}{\epsilon}\partial_z H_y - \frac{1}{\epsilon}\partial_t P_x, \tag{2}$$

where E_x, H_y are the electric and magnetic fields, respectively, and ϵ, μ are the electric permittivity and the magnetic permeability in the medium, respectively. The macroscopic nonlinear polarization $P_x = -N_\mathrm{v}\wp S_1(t)$ is connected with the off-diagonal density matrix element $S_1(t)$, $S_2(t)$, and the population difference $S_3(t)$ between the subbands, which are determined by the effective nonlinear Bloch equations[20]:

$$\partial_t S_1(t) = [\omega_{10} - \gamma S_3(t)]S_2(t) - \frac{S_1(t)}{T_2}, \tag{3}$$

$$\partial_t S_2(t) = -[\omega_{10} - \gamma S_3(t)]S_1(t) + 2[\frac{\wp E_x(t)}{\hbar} - \beta S_1(t)]S_3(t) - \frac{S_2(t)}{T_2}, \tag{4}$$

$$\partial_t S_3(t) = -2[\frac{\wp E_x(t)}{\hbar} - \beta S_1(t)]S_2(t) - \frac{S_3(t)+1}{T_1}, \tag{5}$$

1671-7694/2008/090689-04 © 2008 Chinese Optics Letters

where $S_1(t)$ and $S_2(t)$ are, respectively, the mean real and imaginary parts of polarization and $S_3(t)$ is the mean population inversion per electron (difference of the occupation probabilities in the upper and lower subbands). $\wp$ is the electric dipole matrix element between the two subbands, and N_v is the electron volume density. Also, the nonlinear parameters ω_{10}, β, γ are given by

$$\omega_{10} = \frac{E_1 - E_0}{\hbar} + \frac{\pi e^2}{\hbar \epsilon_r} N_s \frac{L_{1111} - L_{0000}}{2}, \quad (6)$$

$$\gamma = \frac{\pi e^2}{\hbar \epsilon_r} N_s (L_{1001} - \frac{L_{1111} + L_{0000}}{2}), \quad (7)$$

$$\beta = \frac{\pi e^2}{\hbar \epsilon_r} N_s L_{1100}, \quad (8)$$

where ω_{10} is the renormalized but time-independent transition energy, β is the coeffecient of the nonlinear term that renormalizes the applied field due to the induced polarization, and γ is a result of the interplay between vertex and self-energy corrections to the transition energy. The depolarization effects parameters γ and β trace from the nonlinearity arising due to electron-electron interactions on IS transitions in semiconductor QWs. N_s is the electron sheet density, ϵ_r is the relative dielectric constants, e is the electron charge, E_0, E_1 are the eigenvalues of energy for the ground and excited states in the well, respectively, and $L_{ijkl} = \iint \mathrm{d}z\mathrm{d}z' \xi_i(z)\xi_j(z')|z - z'|\xi_k(z')\xi_l(z)$, with $i, j, k, l = 0, 1$. Also, $\xi_i(z)$ is the wave function for the ith subband along the growth direction (z axis). In Eqs. (3)—(5), the terms containing the population decay time T_1 and the dephasing time T_2 describe relaxation processes in the QW and have been added phenomenologically in the effective nonlinear Bloch equations. However, the issue of relaxation is a difficult one and is closely related to the extension of the proposed wave function to include correlations and the interaction with phonons. If there is no relaxation in the system T_1, $T_2 \to \infty$, then $S_1^2(t) + S_2^2(t) + S_3^2(t) = 1$.

Next, we will discuss the impact of the propagation effects on the IS Rabi flopping in multiple GaAs/AlGaAs symmetric double QWs, on the basis of the numerical solutions of the full wave Maxwell-Bloch equations [Eqs. (1)—(5)]. The unit of the system consists of two GaAs symmetric square wells of 5.5-nm width and 219-meV height. The wells are separated by an $Al_{0.267}Ga_{0.733}As$ barrier of $d' = 1.1$-nm width. The structure of the multiple QWs contains $N = 40$ equally spaced units with separation $d = 20$ nm. Then, the system parameters, which dependent on N_s, can be calculated. For an example, the electron sheet density is taken to be $N_s = 1.0 \times 10^{11}$ cm^{-2}, and the electron volume density is $N_v = N_s/L$, where L is the well width. Then the parameters are calculated to be $E_1 - E_0 = 44.955$ meV, $\pi e^2 N_s (L_{1111} - L_{0000})/2\epsilon_r = 0.206$ meV, $\hbar\gamma = 0.0475$ meV, and $\hbar\beta = -0.78$ meV. The dipole moment for the structure is $\wp = -32.9e \times 10^{-10}$ m. In addition, as the dephasing is the crucial relaxation process in semiconductor QWs, we choose $T_1 = 100$ ps and $T_2 = 10$ ps as in Ref. [20].

We assume that the system is initially in the lowest subband, so the initial conditions are $S_1(0) = S_2(0) = 0$, and the population difference is $S_3(0) = -1$. The system we consider is excited at exact resonance, $\omega = \omega_{10}$, and the width of the ultrashort pulse is $\tau_p = 0.15$ ps. For the following application, we characterize the strength of the electron-light interaction by the pulse area, $\Theta(z = 0) = \int_{-\infty}^{\infty} \frac{\wp}{\hbar} E_x(z = 0, t')\mathrm{d}t' = \Omega_0 \tau_p \pi/1.76$, where $\Omega_0 = -\wp\varepsilon_0/\hbar$ is the peak of the Rabi frequency.

To determine the impact of propagation effects, we investigate the temporal behavior of the population difference $S_3(t)$ in QWs, with and without propagation effects, respectively. To characterize the case without propagation effects, we focus on the response of a single double symmetric QWs only by solving the nonlinear Bloch equations (Eqs. (3)—(5)). With a π ultrashort pulse, we show the time evolution of the population difference $S_3(t)$ between the two subbands with different smaller densities in Fig. 1(a). From the results presented, the electrons are almost excited to the upper subband, and an almost complete electron transfer is achieved in the absence of propagation effects. The changes of the electron sheet density scarcely have any impact on dynamics of electrons, i.e., the nonlinearities arising from electron-electron interactions can be negligible with smaller electron densities.

Then, we consider the system with 40 double QWs and take the propagation effects into account. By solving the Maxwell-Bloch equations (Eqs. (1)—(5)) with finite-difference time-domain (FDTD) method[22−24], we show the time evolution of population difference $S_3(t)$ with π pulses for different N_s in Figs. 1(b) and (c). The behavior of the population difference is quite different from that of the single double QWs. In the presence of propagation effects, the electrons are excited to the upper subband in each QWs, but they soon almost return to the lowest subband subsequently. The population difference $S_3(t)$ have different behaviors for different electron densities N_s and the lifetime of electrons in the excited subband becomes shorter as the increase of N_s.

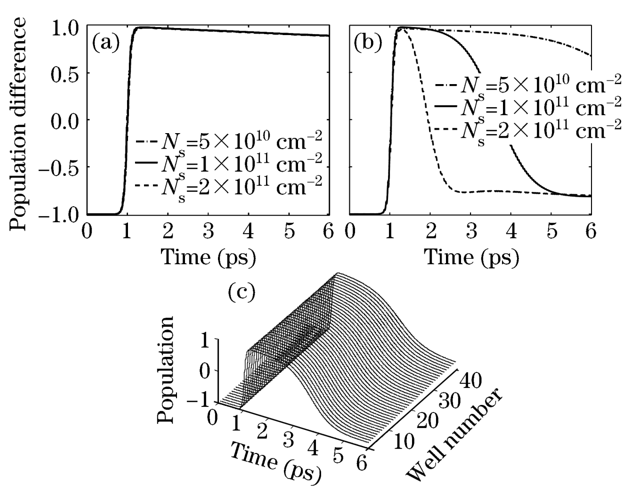

Fig. 1. Time evolution of the population difference, $S_3(t)$, with π pulse [$\Theta(z = 0) = \pi$] for different densities. (a) In a single double symmetric QWs without propagation effects; (b) at the input surface of the multiple QWs with propagation effects; (c) in each double QWs of $m = 40$ with propagation effects for the carrier density $N_s = 1.0 \times 10^{11}$ cm^{-2}.

This physical mechanism of the above phenomenon can be understood as follows. With the propagation of pulse in the system, the incident electric field $E_x(z,t)$ in the QWs creates a transient IS polarization P_x, which in turn coherently emits electromagnetic fields[18]. Due to the strong reemitted fields contributions, the local electric field exhibits strong temporal and spatial dependence. And the reemitted fields lead to a modification of the local electric field, which is not equal to the incident field. This modification is the cause of the radiative coupling phenomena due to propagation effects, which has large impact on the IS Rabi flopping and reduces similarity to the two-level systems drastically. Moreover, considering the Maxwell-Bloch equations, the polarization $P_x = -N_\mathrm{v}\mu S_1(t)$ is related to the electron density N_v and the off-diagonal density matrix element $S_1(t)$. Therefore, with the increase of N_s, the reemitted fields become comparable to the incident pulse, and the interference of the fields reduced the contributions to exciting the electrons to the upper subband. Thus, the electrons decay to the ground state quickly after the incident pulse (Figs. 1(b) and (c)). It is shown that the changes of N_s have obvious effect on the time evolution of population difference $S_3(t)$ in the present of propagation effects. However, due to the small electron sheet densities above, the spatial dependence of the local field is so feeble that the population difference in each double QWs has the same dynamic behaviors (Fig. 1(c)).

Furthermore, we present the temporal behavior of population difference $S_3(t)$ with much larger electron density $N_\mathrm{s} = 5.0 \times 10^{11}$ cm^{-2} in Fig. 2 and other larger electron densities which are now shown here. Under this condition, the nonlinear parameters γ, β, which become comparable to Rabi frequency Ω_0, introduce the time dependence of the transition energy and effective Rabi frequency. Therefore, the complete population inversion is also not possible in a single double QWs due to the strong electron-electron interactions (Fig. 2(a) (the dashed line)). However, we can use a pulse which is suitably chirped (time-dependent carrier frequency) to track self-consistently the renormalized subband splitting in time induced by the pulse itself[21]. While in the presence of propagation effects, due to both strong internal field and the strong nonlinearity arising from the macroscopic number of electrons, the local electrical field exhibits strong spatial dependence. In the first QWs, the electrons are almost excited to the upper subband, even the external field has almost decayed, reemitted field contributions are strong enough to excite electrons into the upper subband (Figs. 2(a) and (b)). While the populations in the subsequent QWs are predominately in the lower subband as the the electric field weakens.

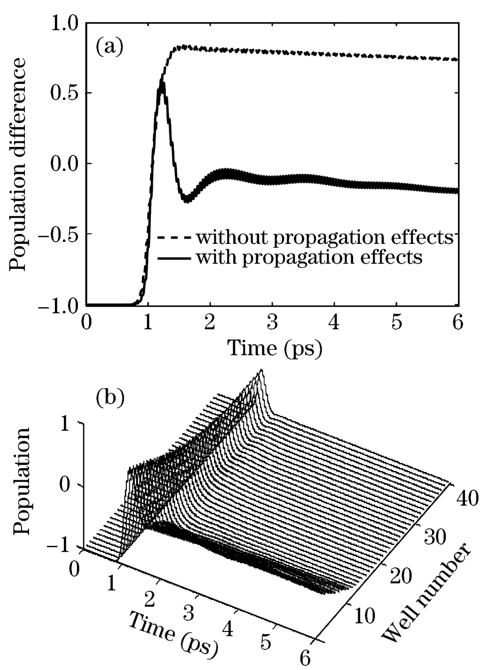

Fig. 2. Time evolution of the population difference, $S_3(t)$, with π pulse $[\Theta(z=0)=\pi]$ for the carrier density $N_\mathrm{s} = 5.0 \times 10^{11}$ cm^{-2}. (a) The case of dashed line is in a single double symmetric QWs without propagation effects and the solid line is at the input surface of the multiple QWs with propagation effects; (b) in each double QWs of $m = 40$ with propagation effects.

In conclusion, we present that the propagation effects have larger impact on IS Rabi flopping in multiple semiconductor QWs compared with the nonlinearities rooted from electron-electron interactions, by solving the Maxwell-Bloch equations with π ultrashort pulses. With smaller electron sheet density, the electrons can be excited completely to the upper subband in a single double QWs; while for the multiple QWs with propagation effects, the electrons almost decay to the lower subband after the ultrashort pulses, no complete population inversion in achieved. Moreover, due to the small internal field, the Rabi flopping in each double QWs is similar. In contrast, due to large carrier density, the complete population inversion is impossible, and propagation effects yields distinctively different population excitation behaviors in the different wells. Therefore, the magnitude of the impact of propagation effects may be controlled by varying the carrier density.

This work was supported by the National Natural Sciences Foundation of China under Grant No. 60708008. N. Cui is the author to whom the correspondence should be addressed, her e-mail address is cuinicn@siom.ac.cn.

References

1. I. I. Rabi, Phys. Rev. **51,** 652 (1937).
2. I. I. Rabi, Phys. Rev. **53,** 318 (1938).
3. S. T. Cundiff, A. Knorr, J. Feldmann, S. W. Koch, and E.-O. Göbel, Phys. Rev. Lett. **73,** 1178 (1994).
4. L. Allen and J. H. Eberly, *Optical Resonance and Two-Level Atoms* (Academic, Dover, New York, 1987).
5. R. Binder, S. W. Koch, M. Lindberg, N. Peyghambarian, and W. Schäfer, Phys. Rev. Lett. **65,** 899 (1990).
6. M. Saba, F. Quochi, C. Ciuti, D. Martin, J. Staehli, and B. Deveaud, Phys. Rev. B **62,** R16322 (2000).
7. A. Knorr, Th. Östreich, K. Schönhammer, R. Binder, and S. W. Koch, Phys. Rev. B **49,** 14024 (1994).
8. S. Hughes, W. Harshawardhan, and D. S. Citrin, Phys. Rev. B **60,** 15523 (1999).
9. A. Schülzgen, R. Binder, M. E. Donovan, M. Lindberg, K. Wundke, H. M. Gibbs, G. Khitrova, and N. Peyghambarian, Phys. Rev. Lett. **82,** 2346 (1999).
10. G.-Y. Slepyan, A. Magyarov, and S. A. Maksimenko, Phys. Rev. B **70,** 045320 (2004).

11. S. Stufler, P. Machnikowski, P. Ester, M. Bichler, M. Axt, T. Kuhn, and A. Zrenner, Phys. Rev. B **73,** 125304 (2006).
12. E. Paspalakis, M. Tsaousidou, and A. F. Terzis, J. Appl. Phys. **100,** 044312 (2006).
13. A. A. Batista and D. S. Citrin, Phys. Rev. Lett. **92,** 127404 (2004).
14. A. A. Batista and D. S. Citrin, Phys. Rev. B **74,** 195318 (2006).
15. C. W. Luo, K. Reimann, M. Woerner, T. Elsaesser, R. Hey, and K. H. Ploog, Phys. Rev. Lett. **92,** 047402 (2004).
16. T. Müller, W. Parz, G. Strasser, and K. Unterrainer, Phys. Rev. B **70,** 155324 (2004).
17. T. Stroucken, A. Knorr, P. Thomas, and S. W. Koch, Phys. Rev. B **53,** 2026 (1996).
18. T. Shih, K. Reimann, M. Woerner, T. Elsaesser, I. Waldmüller, A. Knorr, R. Hey, and K. H. Ploog, Phys. Rev. B **72,** 195338 (2005).
19. I. Waldmueller, W. W. Chow, and A. Knorr, Phys. Rev. B **73,** 035433 (2006).
20. A. Olaya-Castro, M. Korkusinski, P. Hawrylak, and M.-Y. Ivanov, Phys. Rev. B **68,** 155305 (2003).
21. E. Paspalakis, M. Tsaousidou, and A. F. Terzis, Phys. Rev. B **73,** 125344 (2006).
22. K. S. Yee, IEEE Transactions on Antennas Propaggation **14,** 302 (1966).
23. R. W. Ziolkowski, J. M. Arnold, and D. M. Gogny, Phys. Rev. A **52,** 3082 (1995).
24. G. Mur, IEEE Transactions on Electronmagnetic Compatibility **EMC-23,** 377 (1981).